

Sulfate-reducing bacteria streamers and iron sulfides abruptly occlude porosity and increase hydraulic resistance in proppant-filled shale fractures

Bruce W. Fouke, Ananda S. Bhattacharjee, Glenn A. Fried, Mayandi Sivaguru, Robert A. Sanford, Lang Zhou, Reinaldo E. Alcalde, Kenneth Wunch, Amber Stephenson, Joseph A. Ferrar, Alvaro G. Hernandez, Chris Wright, Christopher J. Fields, Lauren G. Todorov, Kyle W. Fouke, Cyrus M. Bailey, and Charles J. Werth

AAPG Bulletin, v. 106, no. 1 (January 2022), pp. 179–208

Copyright ©2022. The American Association of Petroleum Geologists. All rights reserved.

MATERIALS AND METHODS

To investigate the sulfate-reducing bacteria (SRB) biofilm growth during fracking within the Devonian New Albany Shale Formation within the southernmost Illinois Basin (detailed geological setting presented within the main text), a real-rock shale GeoBioCell (GBC) microfluidic testbed was designed and operated. A handheld diamond glass cutter (Ted Pella Inc., Redding, California) was used to cut two standard-sized glass biology slides (25 × 75 mm, VWR, United States) down to a length of 60 mm. Two 8-mm-long notches were then cut into the ends of each of these shortened (60 mm) glass slides with the MK-101-24 tile saw (Figure 2A, main text). Two of these shortened and notched glass slides were epoxied to a standard-sized glass biology microscope slide, forming a stack of epoxied slides (EA E-30CL, Loctite) (Figure 2A, main text). Two 22 × 60-mm glass coverslips (No. 1.5, VWR) were then epoxied on top of this stack of glass slides such that only the outermost 5-mm margin of the face was covered (Figure 2A, main text). A billet of the New Albany Shale was then cut into four pieces, including a triangular inlet end piece, a small rectangular outlet piece, and two other pieces (one of which was shorter than the other by 4 mm), forming the sides of the inlet channels and the primary microfluidic channel. The faces along the length of the microchannel were polished on 600 grit EcoMet 250 lap wheel on a PetroThin thin-sectioning system (Buehler, Chicago, Illinois). The ~500- μm width of the primary experimental microchannel was created by securing two 250- μm -thick sheets of paper between the two

individual shale pieces with a low-temperature melting wax (Electron Microscopy Sciences, Hatfield, Pennsylvania). The paper is aligned, leaving ~2 mm from the bottom surface of the shale pieces. Additionally, a 100- μm -thick paper was used as a spacer to hold the rectangular piece against the longer shale piece with wax. Reduction of the microchannel width to 100 μm prevented loss of proppants from the outlet port. This shale-paper-shale assemblage was then polished on 600 grit (as mentioned above) and epoxied to the top of the stack of epoxied glass slides while using the offset cover slip as a positioning guide (Figure 2B, main text). Two glass cover slips were then epoxied on the other side of the shale assemblage. The shale billet attached to the glass slides was mounted on a Buehler PetroThin thin-sectioning system. An ~450- μm -thick section (measured from the surface of the top slide) was cut using an 8 × 0.0045-in. diamond blade (Buehler Continuous Rim Diamond Blade) mounted on a PetroThin thin-sectioning system. Four pieces of polyetheretherketone (PEEK) tubing, each 14 cm long and having a 1/8-in. outside diameter and 0.030-in. inside diameter (Part No. 1533XL, IDEX, Oak Harbor, Washington), was then epoxied into the notches on each end of the stack of epoxied glass slides, ensuring that the epoxy was raised to a level above the shale assemblage. The surface of the attached shale assemblage was then polished using a series of lap wheel abrasives that ranged from 400 grit paper to 15- μm diamond polish (Buehler) using the glass coverslips as guides. Polishing removed dried epoxy and uniformly leveled the surface of the shale and epoxy. A 22 × 60-mm glass cover slip was epoxied

across the top. In addition, standard-sized glass biological slides were cut to a length of 15 mm and epoxied to the surface of each end of the GBC to reinforce the coverslips over the tubing and hold the GBC identification number (Figure 2D, main text). Throughout the construction process, considerable care was taken to prevent epoxy from entering and blocking the microchannel, PEEK tubing, and insertion notches (Figure 2D, main text).

GENOMIC SEQUENCING AND BIOINFORMATIC ANALYSES

The care and handling of the Dupont SRB enrichment culture used in the shale GBC experimentation is described in detail in the main text. Composition of

the growth medium used for the DuPont SRB enrichment culture is presented in Table S1. Multiple bioinformatic strategies were used to analyze the resulting genomic sequence data. Raw reads (2×250 bps Pro-Glu paired-end gene families [PE]) from the NovaSeq 6000 platform were quality filtered (QF) with the Trimmomatic v0.32 (Bolger et al., 2014) program using parameters: phred33 LEADING:0 TRAILING:5 SLIDINGWINDOW:4:15 MINLEN:36. The low-complexity reads were removed by bbdup.sh, a BBTools suite computational package with a threshold of 0.5 (entropy). The de novo assembly of the QF reads was performed using metaSPAdes v3.11.1 (Bankevich et al., 2012) using the following parameters: `-phred-offset 33, -meta`. The per base coverage across the assembled contigs was calculated by mapping QF reads against the contiguous surfaces using bbmap.sh of

Table S1. Composition of the Growth Medium Used for the Dupont Sulfate-Reducing Bacteria Enrichment Culture

Mineral Salts 100× Stock Solution	For 100 ml (100×)	Molarity in Final Media Solution
CaCl ₂ ·2H ₂ O	0.15 g	102 μM
MgCl ₂ ·6H ₂ O	0.20 g	98 μM
FeSO ₄ ·7H ₂ O (alternative)	70 mg (30 mg)	25 μM (10 μM)
Na ₂ SO ₄	50 mg	35 μM
Trace Metal 1000× Stock Solution	For 100 ml (1000×)	Molarity in Final Media Solution
MnCl ₂ ·4H ₂ O	0.50 g	25 μM
H ₃ BO ₃	50 mg	8 μM
ZnCl ₂	50 mg	3.4 μM
CoCl ₂ ·6H ₂ O	50 mg	2.1 μM
NiSO ₄ ·6H ₂ O	50 mg	1.9 μM
CuCl ₂ ·2H ₂ O	30 mg	1.8 μM
NaMoO ₄ ·2H ₂ O	10 mg	0.4 μM
Selenium-Tungsten 1000× Stock Solution	For 100 ml (1000×)	Molarity in Final Media Solution
Na ₂ SeO ₄	0.30 mg	0.0159 μM
Na ₂ WO ₄	0.80 mg	0.0272 μM
Resazurin 2000× Stock Solution	For 100 ml (2000×)	Molarity in Final Media Solution
Resazurin	0.10 g	2.18 μM
Potassium Phosphate Buffer 200 mM	For 100 ml (100×)	Molarity in Final Media Solution
KH ₂ PO ₄	3.48 g	2 mM
K ₂ HPO ₄	2.78 g	
Ammonium Chloride 2M Stock Solution		Molarity in Final Media Solution
NH ₄ Cl	10.7 g	2 mM
VFA solution*		Final Volume Media Solution
CH ₃ COONa	5.33 g	2 ml/100 ml of Romed media
HCOONa	1.33 g	
C ₄ H ₇ NaO ₂	0.668	
C ₃ H ₅ NaO ₂	0.688 g	
Distilled H ₂ O	100 ml	

*Volatile Fatty Acid (VFA) solution is degassed in serum bottle (Wheaton, Illinois) with analytical grade 100% N₂ gas (Airgas, Radnor, Pennsylvania) for 20 min. The serum bottles are sealed with blue butyl rubber stopper and aluminum seal before sterilization.

BBTools suite package (Bushnell et al., 2017) following parameters 'minid=0.95' and 'ambig=random.' Mapping files from bbmap.sh analysis were subsequently used by MetBAT v2.12.1 to bin contigs into metagenome-assembled genomes (MAGs) based on the "sensitive parameters" (Kang et al., 2015). The quality of recovered MAGs were evaluated using CheckM v2.7.13 by assessing the level of contamination and completeness based on 111 and 43, essential single copy, and 43 unique bacterial and archaeal marker genes, respectively (Parks et al., 2015).

Phylogenetic analysis of the recovered MAGs was accomplished using 43 unique marker genes identified by CheckM v2.7.13. National Center for Biotechnology Information (NCBI), nucleotide basic local alignment search tool (BLAST) analysis with 16S ribosomal RNA (bacteria and archaea) NCBI database was used to identify microorganisms that are phylogenetically close to MAGs. Hundreds of complete genomes for genus *Desulfovibrio*, in addition to microorganisms comprising the top 50 nucleotide BLAST hits, were used for phylogenetic classification. The unique copy maker genes of 100 publicly available genomes closely related to SRB culture MAGs were identified. The concatenated 43 unique marker genes were aligned, and a maximum likelihood tree was generated using RAxML v 8.2.4 (Stamatakis, 2014) with the automatic protein model assignment algorithm (PROTGAMMAAUTO) and 100 bootstraps. Genome annotation of the recovered MAGs was performed using Prokka (Seemann, 2014). Metabolic reconstruction of the MAGs was done using BlastKOALA and GhostKOALA (Kanehisa et al., 2016). The online computational platforms Prokka-predicted proteins from the MAGs were uploaded to the KEGG (Kyoto Encyclopedia of Genes and

Genomes) web service for KO (KEGG orthology) assignments to characterize individual gene functions.

REFERENCES CITED

- Bankevich, A., S. Nurk, D. Antipov, A. A. Gurevich, M. Dvorkin, A. S. Kulikov, V. M. Lesin, S. I. Nikolenko, S. Pham, and A. D. Prjibelski, 2012, SPAdes: A new genome assembly algorithm and its applications to single-cell sequencing: *Journal of Computational Biology*, v. 19, no. 5, p. 455–477, doi:10.1089/cmb.2012.0021.
- Bolger, A. M., M. Lohse, and B. Usadel, 2014, Trimmomatic: A flexible trimmer for Illumina sequence data: *Bioinformatics (Oxford, England)*, v. 30, no. 15, p. 2114–2120, doi:10.1093/bioinformatics/btu170.
- Bushnell, B., (2014), BBTools software package. <http://sourceforge.net/projects/bbmap>.
- Bushnell, B., J. Rood, and E. Singer, 2017, BBMerge – Accurate paired shotgun read merging via overlap.: *PLoS One*, v. 12, no. 10, p. e0185056, doi:10.1371/journal.pone.0185056.
- Kanehisa, M., Y. Sato, and K. Morishima, 2016, BlastKOALA and GhostKOALA: KEGG tools for functional characterization of genome and metagenome sequences: *Journal of Molecular Biology*, v. 428, no. 4, p. 726–731, doi:10.1016/j.jmb.2015.11.006.
- Kang, D. D., J. Froula, R. Egan, and Z. Wang, 2015, MetaBAT, an efficient tool for accurately reconstructing single genomes from complex microbial communities: *PeerJ*, v. 3, p. e1165, doi:10.7717/peerj.1165.
- Parks, D. H., M. Imelfort, C. T. Skennerton, P. Hugenholtz, and G. W. Tyson, 2015, CheckM: Assessing the quality of microbial genomes recovered from isolates, single cells, and metagenomes: *Genome Research*, v. 25, no. 7, p. 1043–1055, doi:10.1101/gr.186072.114.
- Seemann, T., 2014, Prokka: Rapid prokaryotic genome annotation: *Bioinformatics (Oxford, England)*, v. 30, no. 14, p. 2068–2069, doi:10.1093/bioinformatics/btu153.
- Stamatakis, A., 2014, RAxML version 8: A tool for phylogenetic analysis and post-analysis of large phylogenies: *Bioinformatics (Oxford, England)*, v. 30, no. 9, p. 1312–1313, doi:10.1093/bioinformatics/btu033.

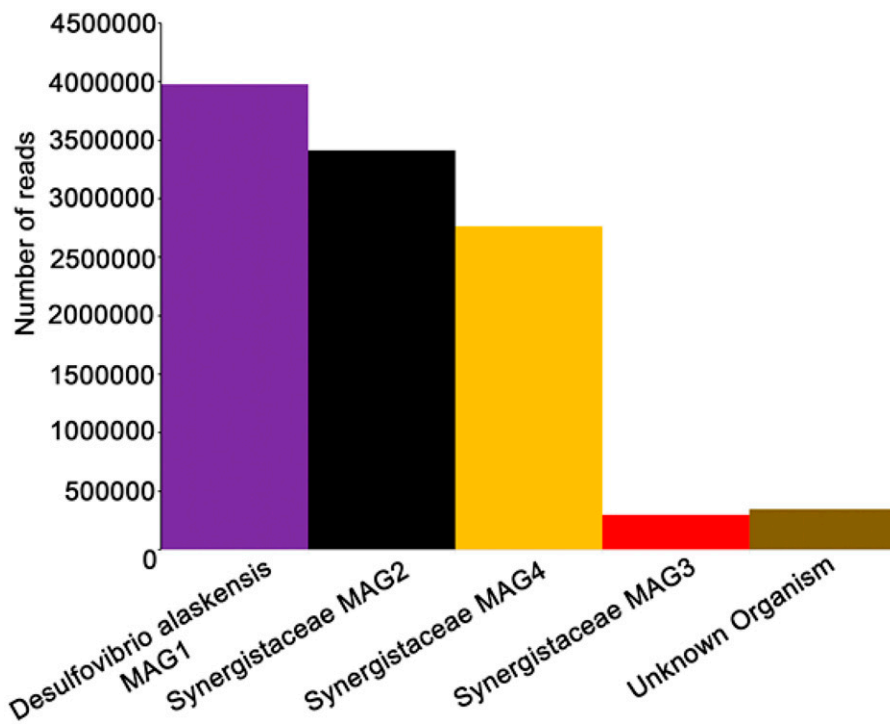


Figure S1. Quality-filtered read abundance plots of the five recovered metagenome-assembled genomes (MAG) from the DuPont sulfate-reducing bacteria enrichment culture metagenomic analyses.

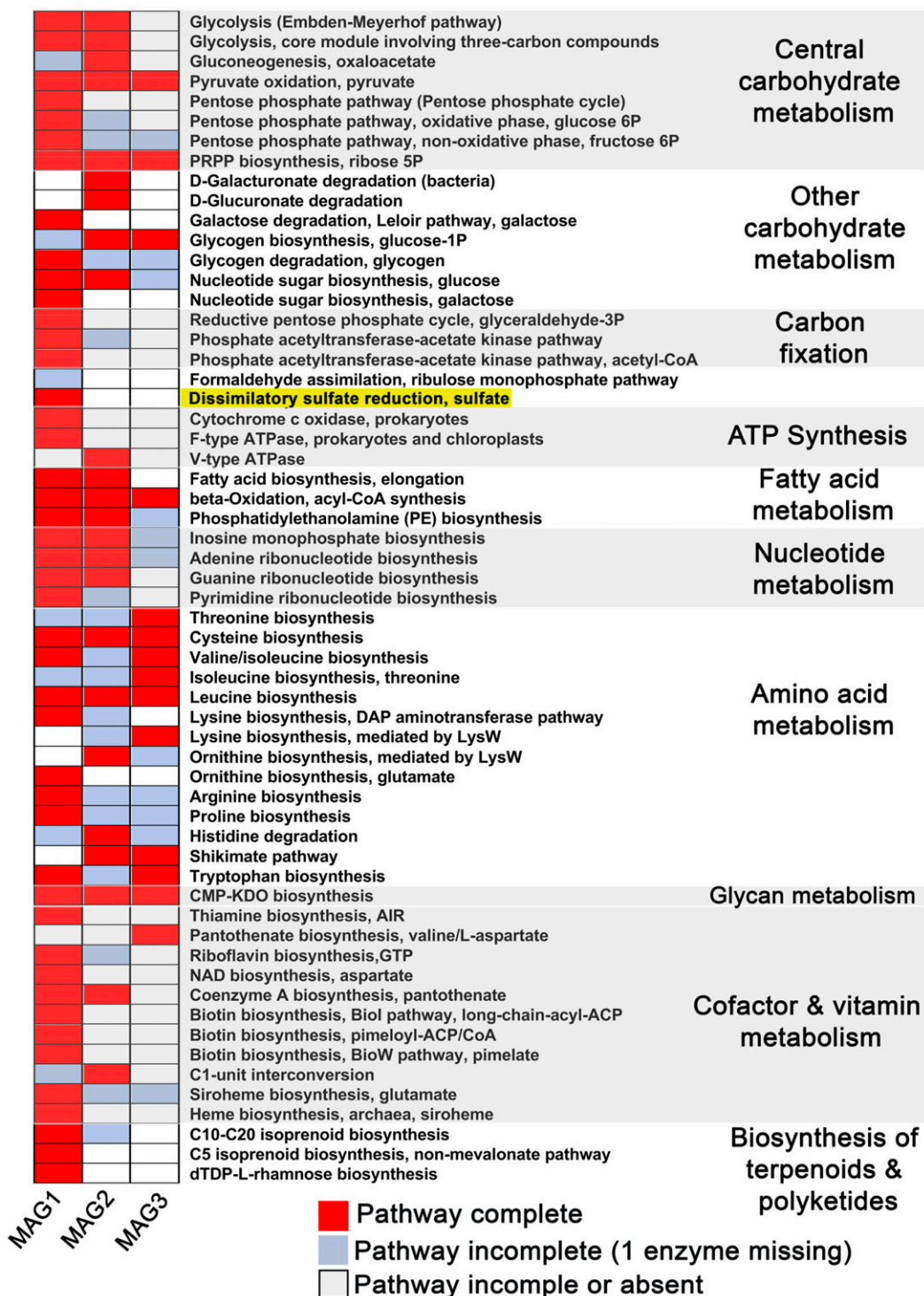


Figure S2. Metabolic pathways encoded by each metagenome-assembled genome (MAG) identified within the Dupont sulfate reducing bacteria (SRB) enrichment culture. Colors represent complete (red), incomplete with 1 enzyme missing (grey), and absent (white) analyses of major metabolic pathways in each identified from the SRB enrichment culture. The dissimilatory sulfate reduction and sulfate pathway is highlighted in yellow.

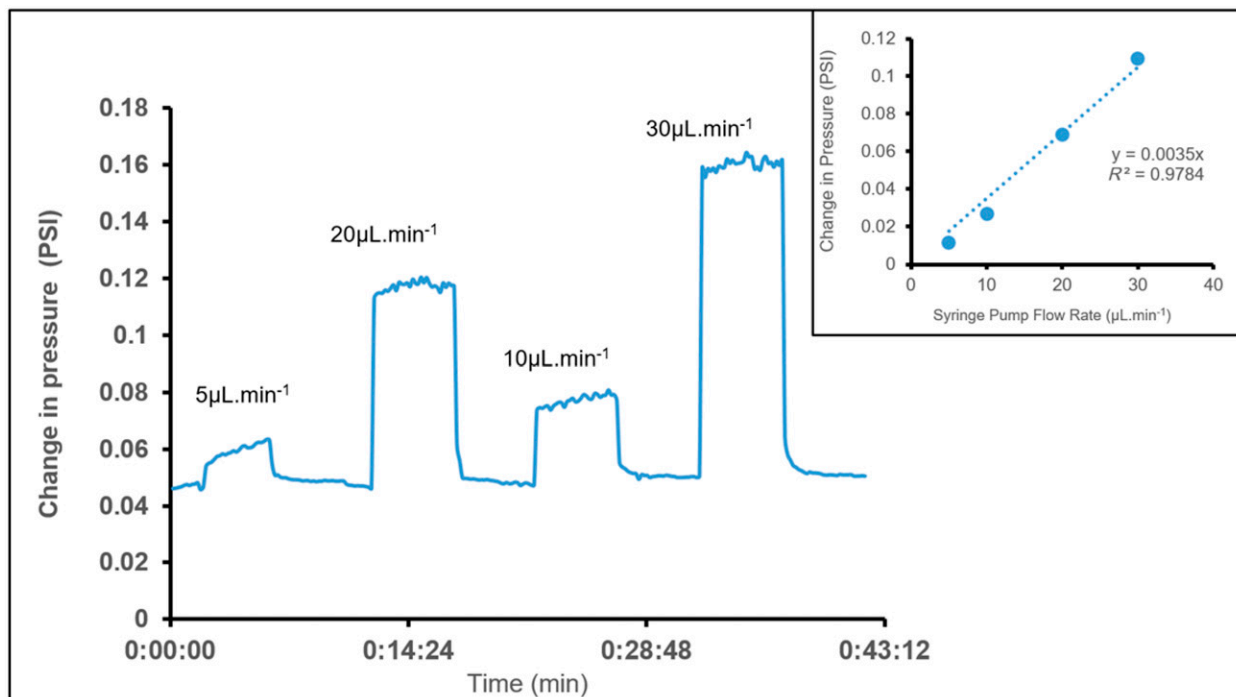


Figure S3. Example cross-plot of shale GeoBioCell experiment duration (Time in minutes) versus change in pressure (PSI). Each plateau represents 300 individual pressure measurements, taken while flow was turned on and off, from which hydraulic resistance is calculated. Inset shows an example cross-plot of syringe pump flow rate ($\mu\text{L}\cdot\text{min}^{-1}$) versus change in pressure (PSI). Each dot represents the average of 300 pressure measurements, with the linear fit forced through the ordinate and abscissa of the axes to define hydraulic resistance. R^2 = coefficient of determination.

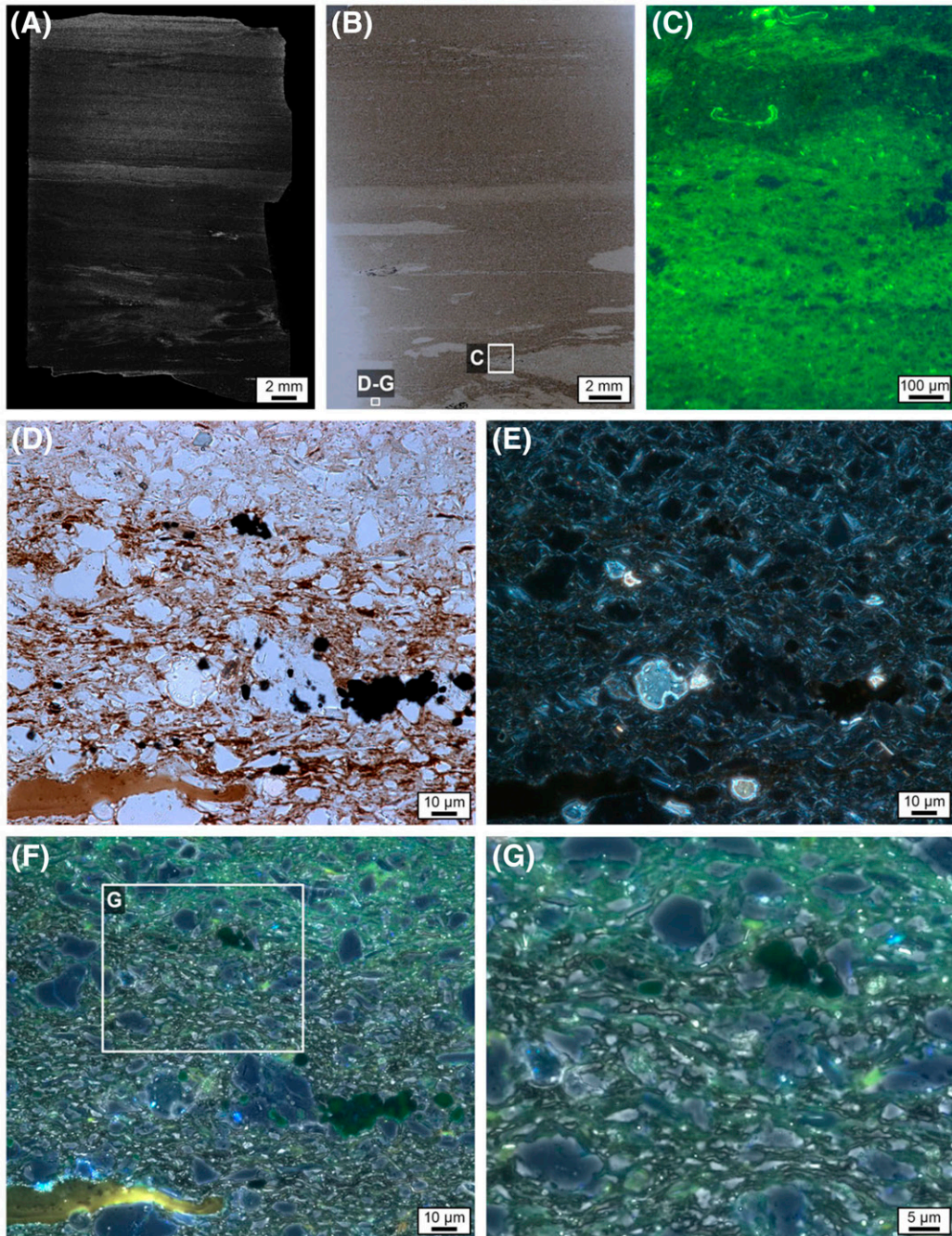


Figure S4. Further development of Figure 3 in the Main Text, presenting additional petrographic analyses of the New Albany Shale sample used to construct the shale GeoBioCell. (A) Contrast adjusted 3D high-resolution X-Ray microCT rendering of a shale billet showing the fine laminated bedding planes and layering. (B) A portion of the same billet shown in (A) where a petrographic thin section (15-20 μm -thick) was made and brightfield (BF) imaged. (C) Enlargement of box in (B), under merged red, green and blue fluorescent light, showing bright Alginite (black). (D) Enlargement of box in (B) showing dark and light brown organic matter layering under high-resolution BF imaging (pyrites are black). (E) Same area as in (D), but under crossed nicols showing most material is amorphous and lacks birefringence. (F) Same location as in (E), showing three-channel wide field autofluorescence (red, green and blue emission channels) merged and overlain on a black and white BF image from the shale thin section (alginite is brightly fluorescence as in (C)). (G) Enlargement of box in (F), illustrating quartz grains (light bluish gray) pyrite crystal aggregates (dark green) and layered organic matter-rich shale (light green).

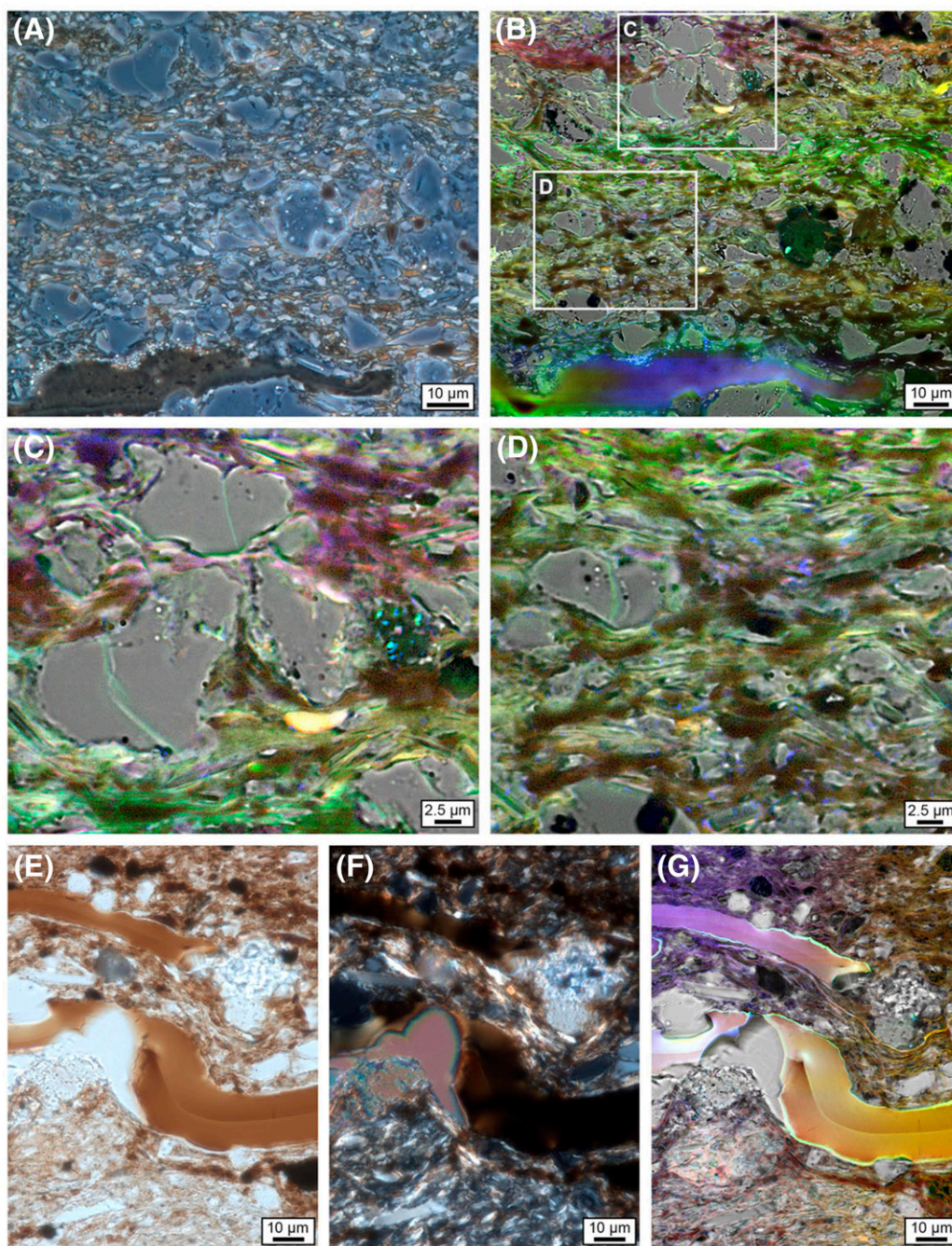


Figure S5. Extension of Figure 3 in the main text, presenting additional petrographic analyses of the New Albany Shale sample used to construct the shale GeoBioCell. (A) Phase contrast brightfield (BF) image of the thin section showing a *Tasmanite* cross-sections composed of alginite near the bottom together with quartz grains (gray grains), pyrite (black grains) and organic matter-rich shale (brown). (B) Same region as (A) but under superresolution autofluorescence (SRAF; merged red, green and blue emission channels using 405, 488, and 568 nm excitation lasers of Airyscan Confocal; 140 nm resolution) showing finely layered multi-color stratigraphic layering of dark brown, green, and light brown colors organic matter (SRAF image merged on a black and white transmitted light brightfield image) of the shale thin section. (C) Enlargement of box in (B) showing porosity (gray) and two to three layers of organic matter with pyrite framboids (cyan color crystals at middle right of the image). (D) Enlargement of box in B showing fine-scale organic matter layering (each with a thickness of 2-3 μm). (E) High-resolution brightfield image of alginites showing dense organic matter undergoing diagenesis. (F) Same location as in (E), under crossed nicols showing only replacement minerals of alginate showing birefringence. (G) Same area as in (F), but under SRAF showing alginites on uneven surfaces indicative of dissolution and reprecipitation (diagenetic alterations). The image is a SRAF merged on a black and white transmitted light BF image of the shale thin section.

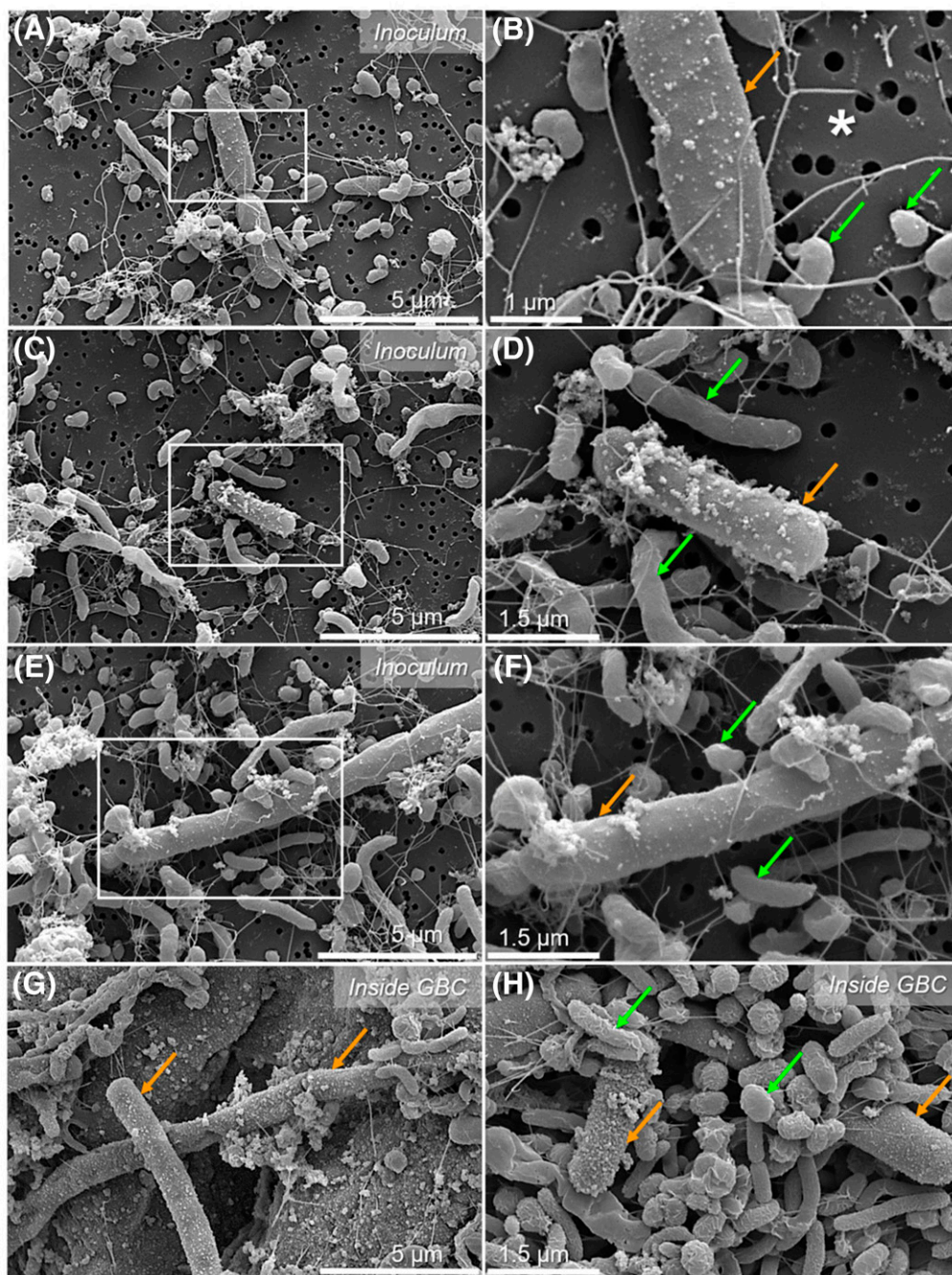


Figure S6. Environmental scanning electron microscope (ESEM) images of cell morphologies comprising sulfate reducing bacteria (SRB) biofilm coatings, streamers, and FeS mineralization in batch culture (A-F) and after inoculation within the shale GeoBioCell (G-H). (A-F) Paired low (A, C, and E) and high-magnification (B, D, and F) from boxes in (A), (C), and (E) showing cells comprising the DuPont SRB enrichment culture containing cells exhibiting rod shaped with round ends (orange arrows), coccoidal shaped and vibrio shaped (green arrows) morphologies grown in batch cultures filtered in 0.2 μm filter (asterisk in B). (G and H) Low (G) and high magnification (H) images of SRB enrichment cultures grown growing 230 h after inoculation within the shale GeoBioCell. Note FeS mineralization confirmed via an energy dispersive spectroscopy (EDS) mounted ion the ESEM, is abundant on the surface of rod shaped bacterial cells with round ends compared to coccoidal shaped and vibrio shaped SRB cells, irrespective of whether they were grown in batch cultures or after injection into the shale GeoBioCell experiments (compare orange arrows vs. green arrows).

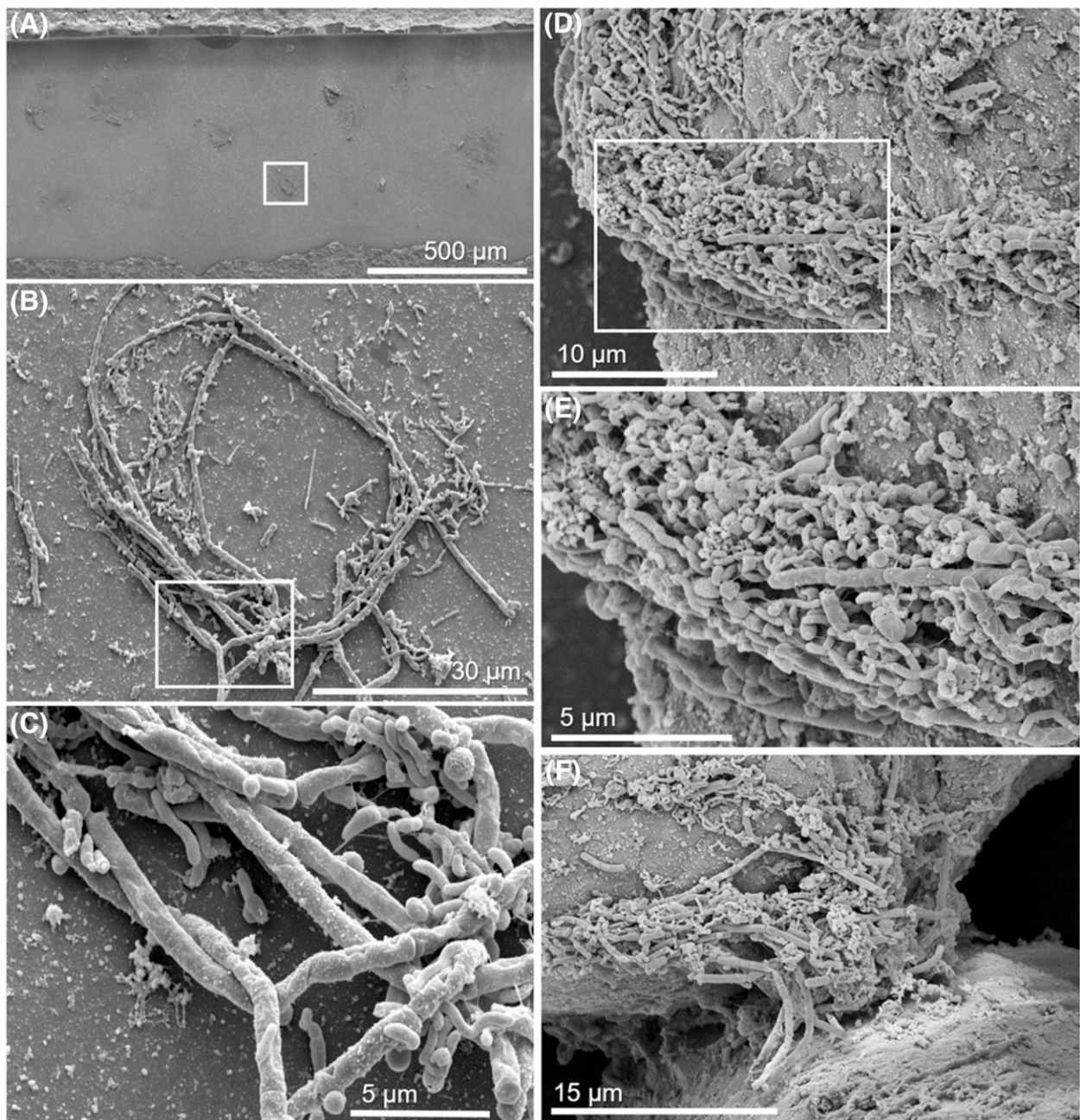


Figure S7. Environmental scanning electron microscope (ESEM) images showing details of biofilm streamer formation and porosity occlusion 230 h after sulfate reducing bacteria (SRB) injection within shale GeoBioCell 1 (NAS-P026) near the inlet area. (A-C) Top surface of the glass covering the shale GeoBioCell 1 showing proppant 'ghosts' where proppants were once touching the inside of the glass covering the microchannel (white boxes). Note the intertwining and coiling nature of SRB rod-shaped cells with round ends (B and C) and extensive FeS biomineralization on their surface. (D-F) SRB biofilm filaments forming the scaffold infrastructure of SRB streamers (D and E) and porosity occlusion by SRB biofilm coatings and streamers on proppants. SRB streamers weave through and around proppants to occlude porosity. These SRB streamers are especially well developed at locations where proppants touch each other (F). NAS = New Albany Shale.

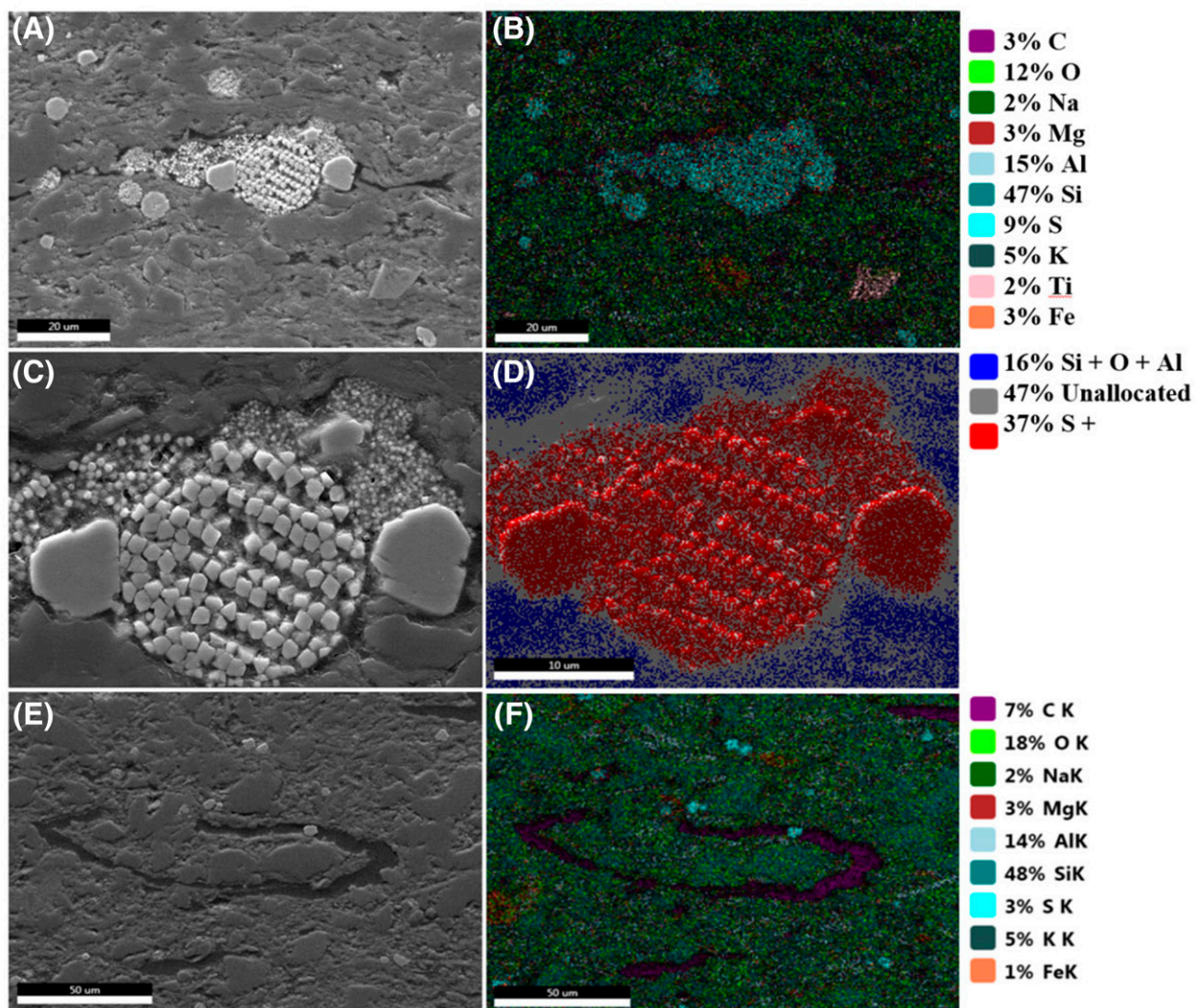


Figure S8. Environmental scanning electron microscope (ESEM) imaging with energy dispersive spectroscopy (EDS) elemental maps of New Albany Shale minerals from billets used to construct the shale GeoBioCell. (A and C) ESEM images (low and high magnification) of polished and etched New Albany Shale billets, as well as from a thin section (E). Their corresponding EDS maps (B, D and F) are pseudo-colored for selected element channels (shown on the right side with weight % compositions).

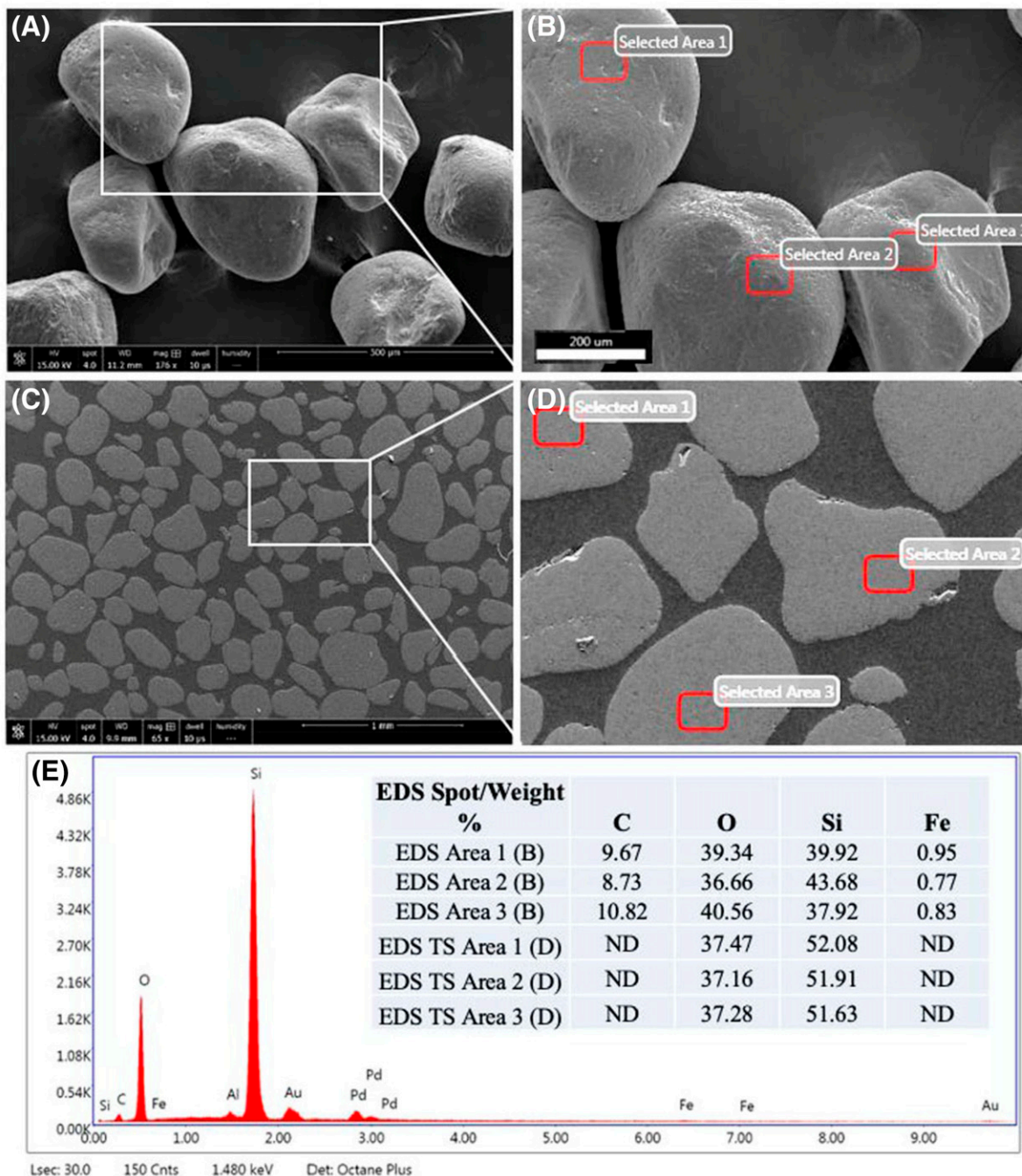


Figure S9. Environmental scanning electron microscope (ESEM) with energy dispersive spectroscopy (EDS) analyses of whole proppants and their thin section, showing their respective elemental compositions. (A-B) Whole proppants attached to the ESEM stub with carbon tape (white box in A enlarged in B) showing three locations where EDS analyses were performed (Area 1-3, red boxes). (C-D) Petrographic thin section of proppants (white box in (C) enlarged in (D)) and three locations where EDS analyses were performed (Area 1-3, red boxes). (E) Representative EDS spectra from Area 1 in B with a table showing elements of interest for all spots and their corresponding weight (%). Cnts = counts; Det = detector; Lsec = live spectral acquisition time in seconds; ND = not determined; TS = thin section.

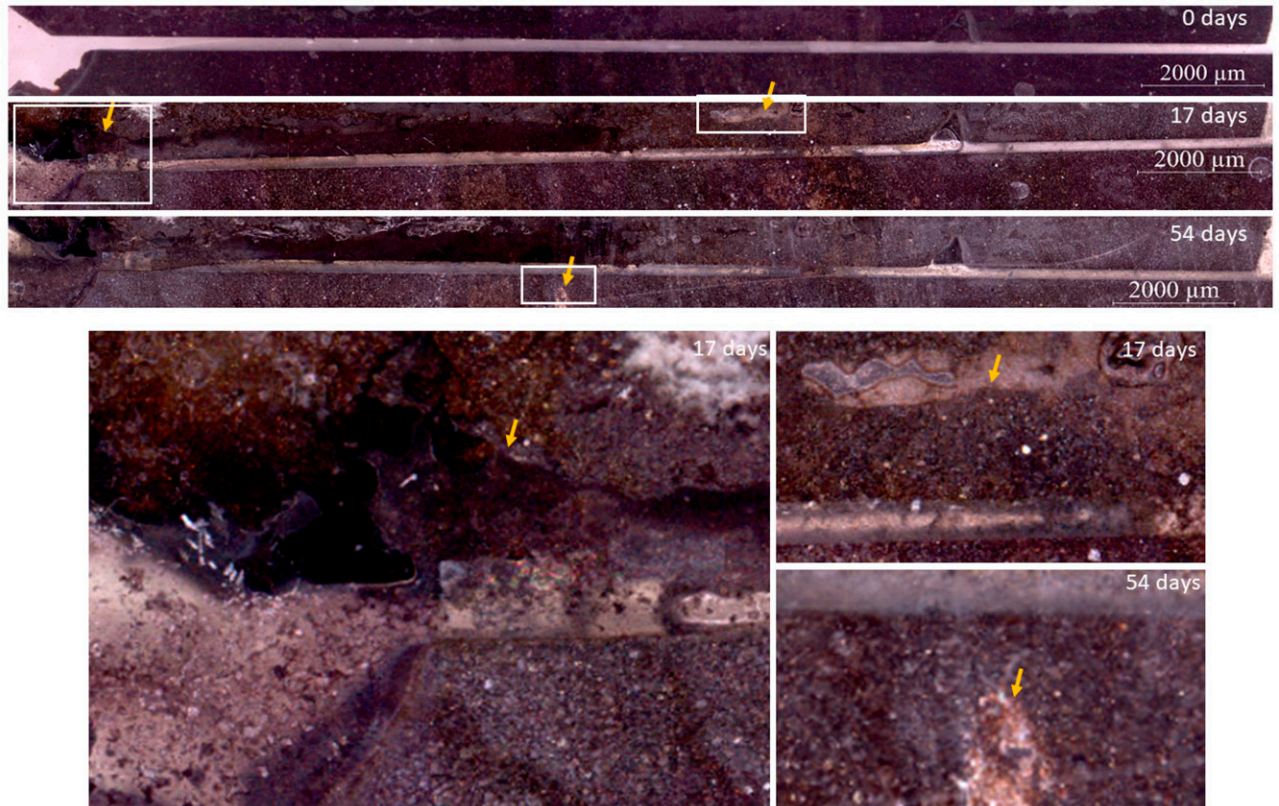


Figure S10. Brightfield (BF) images intact shale GeoBioCell channels operated without proppants. Top photographs are low magnification images of entire New Albany Shale GeoBioCell channels. Bottom photographs are high magnification images of white boxes in top images. Orange arrows indicate shale flaking and chipping due to continuous absorption of water during the course of shale GeoBioCell experimentation. Note comparative integrity of the shale channels walls between 0 days and after 17 and 54 days, respectively. Orange arrows indicate areas of flaking and chipping. See also Video 2 available as AAPG Datashare 141 at www.aapg.org/datashare for time-lapse images with proppant-filled shale GeoBioCell channels exhibiting channel wall flaking and chipping over time.